

High-field autosolitons in photogenerated electron-hole plasma in p-Si

This article has been downloaded from IOPscience. Please scroll down to see the full text article.

2001 J. Phys.: Condens. Matter 13 11623

(<http://iopscience.iop.org/0953-8984/13/50/321>)

View [the table of contents for this issue](#), or go to the [journal homepage](#) for more

Download details:

IP Address: 171.66.16.238

The article was downloaded on 17/05/2010 at 04:41

Please note that [terms and conditions apply](#).

High-field autosolitons in photogenerated electron–hole plasma in p-Si

M Vinoslavskii, A Kravchenko and V Annin

Institute of Physics NASU, 46 Science Ave., 03028, Kyiv, Ukraine

E-mail: mvinos@iop.kiev.ua

Received 26 July 2001, in final form 24 October 2001

Published 30 November 2001

Online at stacks.iop.org/JPhysCM/13/11623

Abstract

Results of experimental observation of high-field thermal-diffusion autosolitons (ASs) in an electron–hole plasma (EHP) in p-Si samples are reported. The EHP was photogenerated by light and heated by an electric field directed along the $\langle 100 \rangle$ axis. It is shown that the EHP is stratified with the formation of a ‘comb’ of five or six static ASs, if the EHP concentration and applied voltage exceed some threshold values, correspondingly. The electric field strength inside the ASs lies between 2000 and 6000 V cm⁻¹, whereas on the outside it spans from 50 to 100 V cm⁻¹. The high strength of the field inside the ASs is caused mainly by the high temperature of the carriers in these domains which may reach up to 1000 K. The multi-valley structure of Si energy bands is qualitatively reflected in both the AS formation dynamics and their further evolution affected by the inter-valley electron transitions in the high-field conditions inside the ASs.

It is well known that for the onset of current instabilities and the generation of self-organized spacial-temporal dissipative structures (DSs) in a monopolar semiconductor plasma under a heating electric field negative N or S type differential conductivity of a crystal is required (see, for example, [1, 2]). In most cases these DSs arise as the current filaments or the electric field domains.

In bipolar semiconductor plasma the DSs can also arise in samples with positive differential conductivity and at much smaller electric fields. In this case the DSs of high amplitude (for example, of either the temperature or concentration of carriers) arise either spontaneously, on the field inhomogeneity in a sample, or under external short-time local carrier heating produced by the electric field or IR radiation absorbed by free carriers. The thermal-diffusion autosolitons (ASs) predicted and described theoretically in [3, 4] also belong to such dissipative structures. Some authors attribute to the existence of such ASs the experimentally observed luminous spots in GaAs films [5], current filaments in reverse-biased p–n junctions in α -SiC [6] and Si p⁺–n⁺–p–n⁻ structures [7], current instabilities stimulated by Joule heating in the InSb

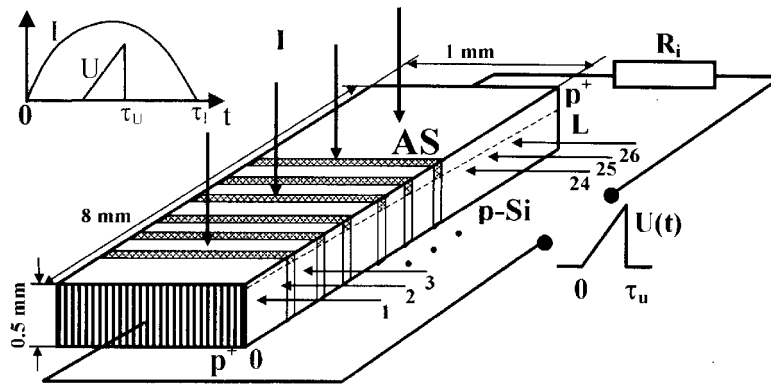


Figure 1. The schematic representation of the setup for measurements of the electric field strength distribution along the sample.

samples [8]. Moreover, the existence of ASs in a photogenerated electron–hole plasma (EHP) in Ge and Si crystals was predicted in the paper [9].

In the past, the high-field thermal-diffusion ASs were studied by researchers in an EHP photogenerated by light and heated by an electric field in n-Ge samples at $T = 77$ K [10–15]. These ASs manifest themselves as narrow strata with a field strength of $E_{AS} = 1000$ – 5000 V cm $^{-1}$ and a carrier temperature of up to $T_e = 1000$ K. The dynamics of formation and subsequent evolution of various types of ASs were investigated depending on crystallographic orientation of the n-Ge samples. In these experiments, generation of static, moving, and pulsating ASs of both single and comb-like types were observed. We attribute such an AS formation mechanism, in accordance with theory [3, 4], to the nonlinear dependence of the electrons' energy relaxation time on their temperature in the vicinity of the Debye temperature.

The interest in AS studies in Si is stimulated by its wide application in semiconductor electronics. However, the mobility of the current carriers in a Si crystal is much lower than that in a Ge crystal, whereas the Debye temperature is higher in Si. This should cause difficulties for AS generation in Si. Consequently, the aim of this work was to determine experimentally the conditions of AS generation in Si crystals.

Samples were cut out as rectangular plates of size $(0.05 \times 0.1 \times 0.9)$ cm 3 from high-resistance p-Si ($\rho \sim 3500$ Ω cm) and were etched in CP-8. The p $^+$ –p Al contacts were fused to opposite smaller end faces of the samples at $T \sim 720$ K. The electric field was directed along the $\langle 100 \rangle$ crystallographic axis. The measurements were carried out at $T = 77$ K. High-density EHP ($n = p = 1 \times 10^{14} - 1 \times 10^{16}$ cm $^{-3}$) was homogeneously photogenerated along the wide facet of the sample using a bell-shaped white light pulse with a duration of $\tau_l \sim 1.5$ ms. Either rectangular or saw-tooth shaped voltage pulse U (duration 0.01–1 ms, amplitude up to 300 V) was applied to the contacts at the top of the light pulse (figure 1). This technique allows one to obtain either the quasi-stationary or dynamic current–voltage characteristics (JVC) at constant sample irradiation and to define the threshold values U_c , at which the nonlinear JVC and DSs occur. The output resistance of the voltage pulse generator was about $R_{out} \sim 0.5$ Ω . This provided a stable voltage, rigid enough over a wide range of current amplitudes (up to 50 A). The single pulses of applied voltage and light were chosen to avoid considerable Joule heating of the sample. The average heating of a sample during a voltage pulse, estimated from the thermal balance equation without account being taken for heat spread into a holder (just as it was done for Ge [14, 15]), did not exceed $\Delta T = 10$ – 20 K.

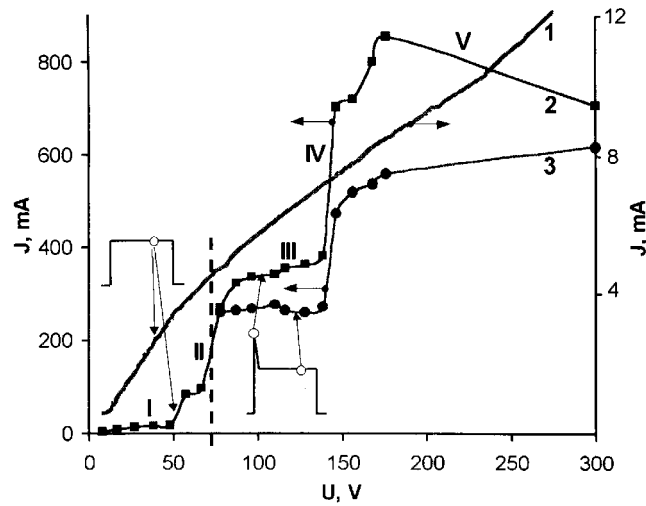


Figure 2. The quasi-stationary current–voltage characteristics (JVCs) of a p-Si sample oriented along the $\langle 100 \rangle$ -axis at $T = 77$ K under non-illuminated (curve 1) and illuminated (curve 2 for the initial current peak and curve 3 for the steady current state) conditions.

The distribution of the electric field strength $E(x)$ along a sample was measured using a microsystem with 26 contact tungsten probes. The spacing between the adjacent probes could be fixed within 0.15–0.4 mm (figure 1). The voltages measured by each pair of the neighbouring probes were registered by two differential inputs of a series of storage oscilloscopes. The oscillograms of local fields $E_{i-j}(t) = \Delta U_{i-j}(t)/l_{i-j}$ in all inter-probe spaces allowed us to plot the distributions of the electric field $E(x)$ along a sample and to determine the AS parameters such as formation time, travel velocity, shape and size.

The quasi-stationary JVC, obtained by using rectangular voltage pulses applied to the non-illuminated Si-samples, is linear with weak diminution of its incline at higher voltages (figure 2, cr. 1). For the JVC of the illuminated Si samples (figure 2, cr. 2,3) we distinguish five specific regions. The first of them (I), measured for $U < 50$ V, is of sublinear dependence. The second (II) and fourth (IV) regions are characterized by the stepped increase of current at $U \sim 75$ and 140 V, accordingly (this is possibly the result of the S-shaped branches of the JVC). The third (III) and fifth (V) regions of JVC are characterized by the current saturation with a trend towards the N-type shape.

To clear the origin of the nonlinearities in both the quasi-stationary and the dynamic JVCs the field distributions along samples, corresponding to distinguished regions of the JVCs, were measured. In the following we will consider three phenomena, which arise in consecutive order when the applied voltage grows and determine the different regions on both the quasi-stationary and the dynamic JVCs: (i) a contact exclusion, (ii) a reversal of direction of the EHP bipolar drift, and (iii) a rise of the high-field ASs.

1. The contact exclusion. At low applied voltages ($U < 50$ V) the contact exclusion process occurs in a sample. The photogenerated EHP travels, due to the bipolar drift, to the positively biased $p^+ - p$ contact in the drift direction of minority carriers—electrons. An exclusion area with reduced-EHP concentration and high electric field strength $E_{0-1}(t) \sim 700$ V cm $^{-1}$ arises near the negatively biased $p^+ - p$ contact, while the high plasma density and low field strength ($E_{2-3} - E_{i-j} = 40 - 50$ V cm $^{-1}$) establish in the rest of the sample (figure 3). This process

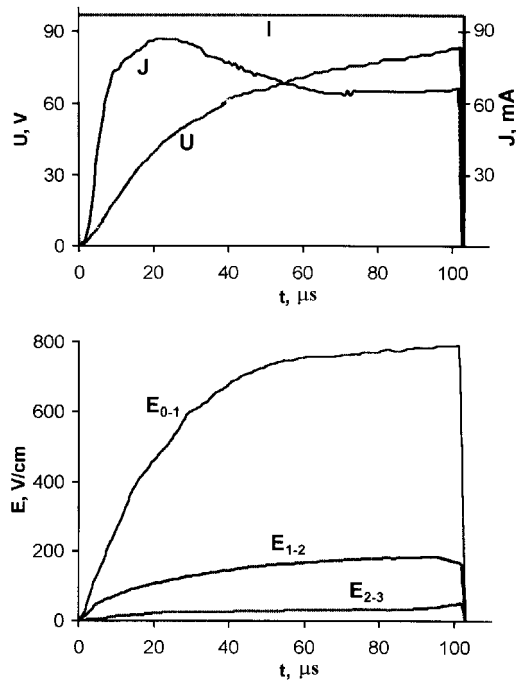


Figure 3. The contact exclusion process at $T = 77 \text{ K}$: the time dependences of the applied voltage U , light intensity $I = \text{const}$, current J and of local electric field strengths at the negatively biased contact E_{0-1} , E_{1-2} , E_{2-3} . Sample 1. $l_{0-1} = 0.35 \text{ mm}$, $l_{1-2} = 0.3 \text{ mm}$, $l_{2-3} = 0.3 \text{ mm}$.

determines the first region (I) of the monotonous current increase with applied voltage in both the quasistationary (figure 2, cr. 2,3) and the dynamic (figure 4) JVCs.

At the beginning of the growth of the saw-tooth applied voltage pulse the field strength $E_{0-1}(t)$ near the contact increases quickly to a high magnitude, and the field strengths in the adjacent regions ($E_{1-2}(t) - E_{4-5}(t)$) grow, with some delay, to far smaller values (figure 3). In the time this process takes the current rises quickly initially and then decreases slowly. This current decrease is caused by both the exclusion area elongation and the Joule heating of a thin layer of the crystal, adjacent to the irradiated surface, in which a bipolar current exists. The thickness of this bipolar conduction layer is determined by the depth of diffusion penetration of photogenerated electrons and holes into the crystal body during the drift time of minority carriers (electrons) along a sample, and may vary from several μm in the exclusion area to several tens of μm near the back contact.

2. The reversal of the bipolar drift direction of the electron-hole plasma. With further magnification of the applied voltage, two step rises of current on the quasi-stationary JVC (figure 2), as well as two current peaks on the dynamic JVC (figure 4), emerge at the threshold voltages U_{c1} and U_{c2} (regions (II) and (IV)). The stepped current rises are accompanied by sharp drops (by 20–30%) of the fields $E_{0-1}(t)$ and $E_{1-2}(t)$ in the exclusion area. This means that the local S-shaped dependence $J(E_{0-1})$ takes place. Such phenomena was not observed earlier for the exclusion process, which is usually characterized by the trend of current saturation with a voltage growth. The whole S-shaped branch appears in the dynamic JVC at higher output resistances of the voltage generator due to small voltage diminution with a steep rise of current.

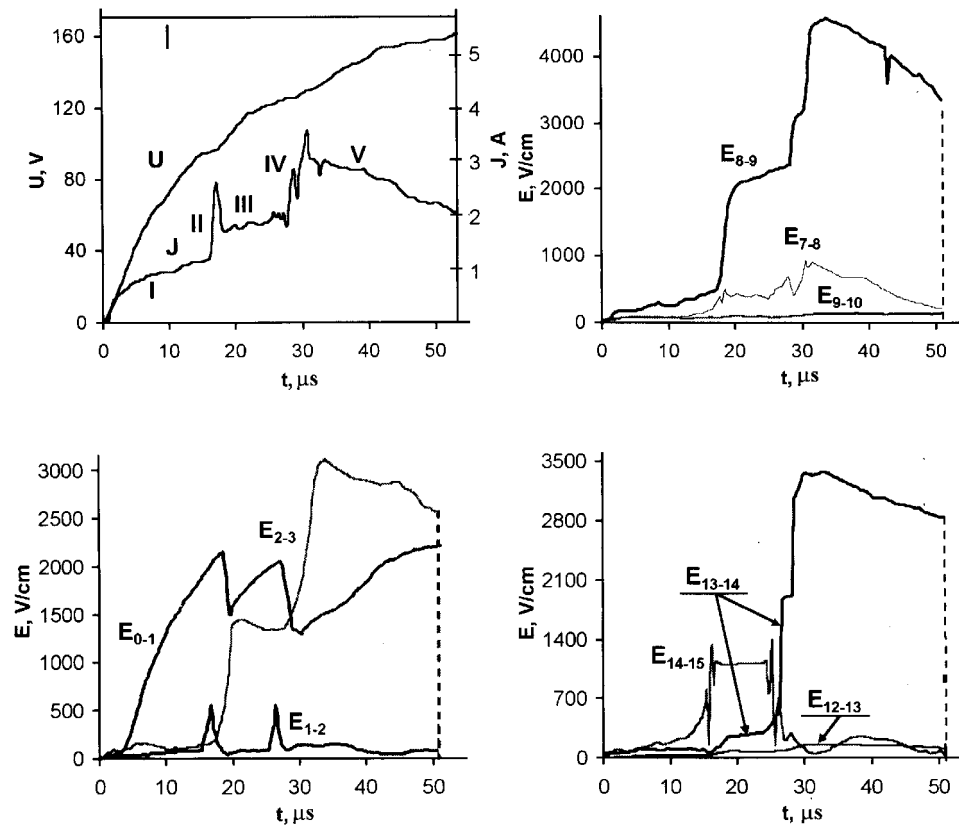


Figure 4. Dynamics of the reversal of the EHP bipolar drift and of formation of the high-field ASs in the sample at $T = 77$ K: the time dependences of the applied voltage U , light intensity $I = \text{const}$, current J and of local field strengths— E_{0-1} —in the exclusion area; E_{2-3} , E_{8-9} , E_{13-14} —in the ASs formation regions; E_{1-2} , E_{6-7} , E_{12-13} , E_{14-15} —outside the AS areas.

We associate the appearance of such S-shaped branches in both the JVCs with a direction reversal of the EHP bipolar drift the origin of which consists of the different field dependence of electron and hole mobilities [16, 17]. In this case the EHP flow is directed from the carrier-enriched low-field area of a sample to the carrier-depleted high-field area near the contact. This EHP flow enhances the carrier density and reduces the field strength in the exclusion region, and causes a steep rise of current (figures 2, 4). After each of the two sharp drops, connected with the bipolar drift reversal, the field $E_{0-1}(t)$ increases monotonously again with applied voltage growth (figure 4), because the EHP drift in the exclusion area aligns again in the direction of the minority carriers (electrons) drift.

The reversal of a bipolar EHP drift was observed also for the p-Si samples at $T = 300$ K. In this case the strong oscillations of the local fields in two neighbouring inter-probe intervals having opposite phases arose at some distance ($\Delta l = 1.5\text{--}2$ mm) from the negatively biased contact (see $E_{4-5}(t)$ and $E_{5-6}(t)$, figure 5) as well as at $T = 77$ K (see figure 4(b), curve $E_{0-1}(t)$). However, the sharp current increase and the S-shaped branch of JVC were absent because the bipolar drift reversal occurred in a low-field area and did not affect the near-contact high-field exclusion area, which mainly determines the current magnitude.

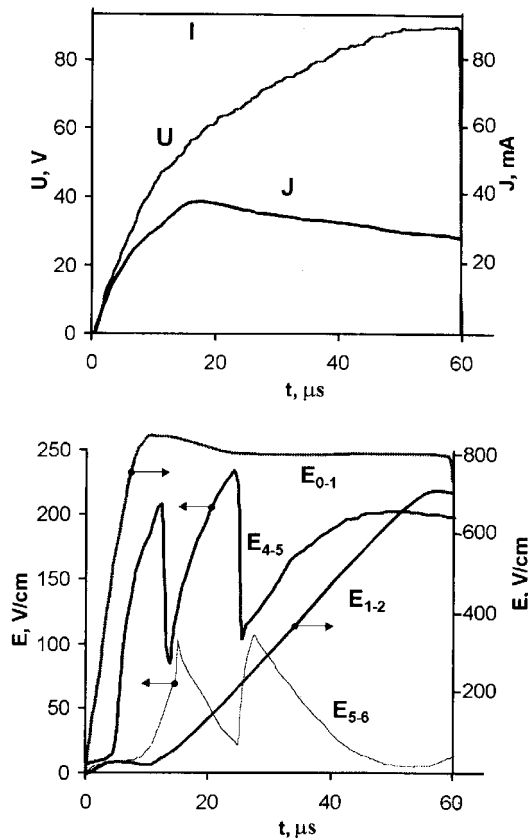


Figure 5. The reversal of the EHP bipolar drift at $T = 300$ K: the time dependences of the applied voltage U , light intensity $I = \text{const}$, current J and of local field strengths— E_{0-1} , E_{4-5} , E_{5-6} .

3. Generation of high-field ASs. The occurrence of the branches (III) and (V), which are characterized by either a current saturation or a weak current decrease (N-shaped dependence) on both the quasi-stationary JVC (figure 2) and the dynamic JVC (after the first and second current peaks, figure 4) at $T = 77$ K, is accompanied by generation and development of some stationary domains of a high field strength ($E_{AS} = 1500\text{--}5000$ V cm $^{-1}$) along a sample. We call these domains high-field thermal-diffusion ASs (figures 4, 6) to conform with theory [4] and experimental results obtained for n-Ge [10, 11].

The first stage of formation of the ASs having a field strength $E_{AS} = 1500\text{--}2000$ V cm $^{-1}$ under a saw-tooth voltage pulse (branch (III) in the dynamic JVC, figures 4, 6, moment t_2) follows immediately after the first current peak and the first abatement of the field $E_{0-1}(t)$ in the exclusion area, where the main portion of voltage initially drops. A decrease of the field $E_{0-1}(t)$ results in an increase in the average field strength in the low-field part of a sample enriched by carriers thus creating proper conditions for generation of the ASs. It should be noted that the initial strong monotonous growth of both the field $E_{0-1}(t)$ and the current at the beginning of the saw-tooth applied voltage pulse, testifies to the exclusion process development (figures 4, 6, moment t_1), but not the AS generation there. In this case AS does not arise near the contact (as it was observed in n-Ge samples earlier [11, 12]) because of low carrier concentration in the exclusion area.

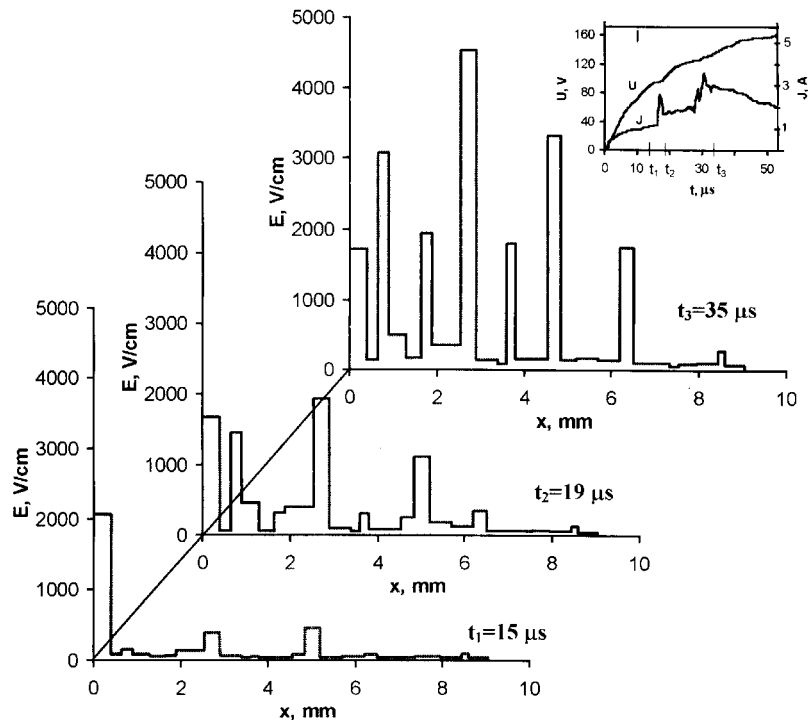


Figure 6. The field strength distributions in the sample at $T = 77$ K in different moments of AS formation during saw tooth voltage pulse: of the contact exclusion process (moment $t_1 = 15 \mu\text{s}$); after the first stage of AS formation (moment $t_1 = 19 \mu\text{s}$); after the second stage of AS formation (moment $t_1 = 34 \mu\text{s}$). The inset shows the shapes of the voltage U and current J pulses during light illumination $I = \text{const}$.

After the second abatement of the field $E_{0-1}(t)$ and the second current peak under the saw-tooth voltage pulse the field strength within the ASs rises sharply once more (1.5–2 times, up to $E_{AS}(t) = 2000\text{--}5000 \text{ V cm}^{-1}$ —branch (V) in the dynamic JVC, figures 4 and 6, moment t_3). The second jump of the AS field in the Si samples in which the field is directed along the $\langle 100 \rangle$ axis is similar to the second AS field jump observed in the n-Ge samples having a field direction along the $\langle 111 \rangle$ axis [12, 14]. In both cases the field direction coincides with the valley axis corresponding to large effective electron mass.

Further augmentation of the saw-tooth voltage leads to multiplication of the generated ASs until they do fill almost all the sample length with a distance interval of about the bipolar drift length ($L_{dr} \sim 1\text{--}1.5 \text{ mm}$) (figure 6, moment t_3). In some regions of the sample the AS formation was accompanied by a 2–3 stepwise increase of the E_{AS} field (figure 4) because of the superposition of several additional steps on the first or second basic steps of the AS field growth. An augmentation of light intensity results in a rise of the AS amplitude near the contact and to its diminution far from the contact. Decrease of illumination leads to growth of the AS amplitude in the middle part of a sample due to a field rise outside the exclusion area.

We can conclude that both the quasi-stationary and the dynamic JVC of illuminated p-Si samples have similar specific branches. The first JVC branch of monotonous current growth corresponds to the contact exclusion process. The second and forth S-shaped JVC branches we associate with the repeating reversal of the EHP bipolar drift. The third and fifth JVC regions having either current saturation or N-shaped branches characterize the arise and evolution of the high-field ASs in a sample.

The measurements of the AS field strength and calculations carried out on the basis of the energy balance equation for a many-valley semiconductor at $T = 77$ K [10, 11], show that the electron temperature in the AS area had achieved a value of $T_e \sim 1000$ K and greater, whereas the carrier concentration was lower as compared to the adjoining low-field areas of a sample.

Thus, a ‘comb’ of static ASs forms in photogenerated EHP in p-Si samples if the voltage exceeds the threshold (figures 4, 5, moment t_3). These ASs are characterized by a high local field, high temperature and reduced carrier concentration. The high field inside the AS is, generally, determined by high carrier temperature. The arise of ASs is accompanied by only a small diminution of current—by 10–20%, since the current is already limited by the high-field exclusion area, in which the high field is determined mainly by a low concentration of carriers.

Similar measurements were also carried out on lower-resistance p-Si samples ($\rho \sim 80 \Omega \text{ cm}^{-1}$) of the same geometry at $T = 77$ K. The stepped increase of current and the sharp decrease of an exclusion field near the contact of the illuminated sample arose at higher threshold voltage ($U_c \sim 220$ V) under the saw-tooth voltage pulse. Thus, the S-shaped branch in the dynamic JVC, which we associate with the reversal of the bipolar EHP drift in the exclusion area, also emerges in these samples. However, an arise of the N-shaped JVC branch and the high-field ASs were not observed in these samples in the voltage range used.

In similar experiments on illuminated n-Ge samples at $T = 77$ K the reversal of EHP bipolar drift had been observed for a voltage beneath that required for AS generation. It was also accompanied by a stepped increase of current (S-shaped branch of JVC) and a drop of the field $E_{0-1}(t)$ near the contact. Hence, the reversal of the EHP bipolar drift itself does not result in the formation of ASs and both these phenomena are self-maintained.

According to existing theory [3, 4] a thermal-diffusion high-field AS can arise in a non-equilibrium quasi-neutral EHP if its parameters obey the following three requirements: (i) the strong inequalities either $l_e/L \ll 1$ or $\tau_e/\tau \ll 1$ are true for two carriers’ spatial or temporal characteristic parameters included into equations of balance for streams of both the particles and the energy (l_e and τ_e are the length and relaxation time of the energy, L and τ are the bipolar diffusion length and lifetime of current carriers); (ii) the nonlinear condition $\alpha + s > -1$ is fulfilled, thus providing the positive feed-back to increase the carriers temperature ($\tau_p \sim (T_e)^\alpha$ and $\alpha = d \ln(\tau_p)/d \ln(T_e)$, $\tau_e \sim (T_e)^s$ and $s = d \ln(\tau_e)/d \ln(T_e)$, τ_p is the relaxation impulse time, and T_e is the temperature of the carriers); (iii) the relation $\tau_p \ll \tau_{ee} \ll \tau_e$ (τ_{ee} is the time of inter-electronic collisions) provides a condition for energy control of the current carriers, and the formation of ASs in the form of high-field domains (rather than the current filaments). According to the energy-balance-equation estimations the specified requirements were met in our experiments.

Therefore, the first stage of AS formation in p-Si samples under saw-tooth voltage pulse (figure 4) is characterized by the one-step rise of a local field $E_{i-j}(t)$ in one or several points, up to a high magnitude of $E_{AS} \geq 1500 \text{ V cm}^{-1}$, which is accompanied by a weak abrupt current decrease. It occurs right away after the first abatement of the field $E_{0-1}(t)$ and the first current peak. We connect this stage of AS formation (as well as in n-Ge samples [10–15]) with the nonlinear dependence of the electrons’ energy relaxation time τ_e versus temperature near the Debye temperature (about 730 K for Si). Under electric field heating the electrons in a temperature range beneath the Debye temperature ($T_e < \theta_D$) the τ_p and τ_e time intervals diminish as $\alpha \approx -1/2$ and $s \approx -1/2$, accordingly, hence, $\alpha + s \approx -1$. Under electrons overheating over the θ_D the time τ_p continuously diminishes with $\alpha \sim -1/2$, but the time τ_e already augments, so $s > 0$, $\alpha + s > -1/2$ and the criterion for AS formation is fulfilled. In fact, the $\alpha + s > -1$ criterion is already met as soon as the electrons’ temperature T_e only approaches the θ_D value and the inequality $s > -1/2$ is met. Then even a short-term local heating of electrons by an electric field, according to the theory [4], causes a realization of

positive feedback to increase the electrons' temperature. Thus, the rate of electron-to-lattice energy transfer diminishes, the temperature of the electrons grows, their mobility drops which stimulates growth of a local field, and, at small current variations, even greater heating of electrons. The holes are heated both by an electric field and in collisions with hot electrons, but in the former case the heating is weaker because of considerably smaller hole mobility.

At the second stage of AS formation which occurs immediately after the second current peak and the field $E_{0-1}(t)$ abatement (because of repeated process of reversal of bipolar drift in the exclusion area) the repeated field jump to higher magnitudes of $E_{AS} = 2000\text{--}6000\text{ V cm}^{-1}$ takes place in all the ASs. This is connected with high-field transitions of electrons inside the ASs between equivalent valleys, namely, from valleys of a light effective mass into a valley with a heavy effective mass that results in decrease of the electron mobility, growth of resistance in the AS area and further increase of the E_{AC} field.

The static state of ASs in the investigated p-Si samples could be explained as follows. First, at very small impurity concentration ($N_A \sim 10^{11}\text{ cm}^{-3}$) and high photogenerated carrier concentration ($n \approx p = 10^{14} - 10^{16}\text{ cm}^{-3}$) the EHP becomes almost one in the sample low-field area (outside the exclusion area) and the bipolar drift velocity tends to zero. Second, this trend is also promoted by a stronger heating-up of the more mobile electrons (in comparison with holes), as well as the transition of the electrons from the 'light' valleys into the 'heavy' one in the field E of $\parallel the \langle 100 \rangle$ axis that strongly diminishes the mobility of the electrons and makes plasma more symmetrical. A similar situation was implemented in our experiments with n-Ge samples having field orientation along the $\langle 110 \rangle$ axis, where we also observed a formation of the static ASs' 'comb' [13]. At the same time, in n-Ge $\langle 111 \rangle$ specimens ASs moved in the direction of the holes' drift, and in $\langle 100 \rangle$ specimens they moved in the electron drift direction [14, 15].

In the region of a static AS the crystal can be heated by the current during a voltage pulse to a high temperature of $T = 400\text{--}600\text{ K}$ that results in thermal carrier generation and a decrease of the field in AS (figure 3, curves. E_{3-4} , E_{8-9} , E_{13-12}). Such high heating is explained, firstly, by the high electrical power value $W = J \times E = (4000\text{--}20\,000)\text{ W cm}^{-1}$ dissipated in the AS region and, secondly, by the small thickness of the bipolar conductivity layer close to the irradiated surface, whose thickness varies from several μm in the exclusion area to several tens of μm near the opposite contact.

Thus, the results obtained in this work confirm experimentally the possibility of generation of high-field thermal-diffusion ASs in a non-equilibrium EHP in samples of pure silicon. The local mechanism of their generation is similar to that of AS formation investigated by us previously for Ge samples [10–13]. However, in the Si samples the ASs arise at threshold voltage, which is approximately 1.5 times higher than that observed for Ge samples. The multi-valley energy band structure of silicon, as well as germanium, is qualitatively reflected both in the AS formation dynamics and in their further behaviour.

Acknowledgments

The authors acknowledge fruitful discussions with and the interest shown by Professor O Sarbei from the Institute of Physics, Kyiv, Ukraine.

This work was supported by the State fund of fundamental researches (grant no 2.4/816), International scientific fund CRDF (grant no UPI-368) and the Ukrainian–Israeli scientific project (grant no 2M/1807-97).

References

- [1] Bonch Bruevich V L, Zvyagin I P and Mironov A G 1981 *Domain Electrical Instabilities in Semiconductors* (Oxford: Pergamon)
- [2] Scholl E 1987 *Nonequilibrium Phase Transitions in Semiconductors* (Berlin: Springer)
- [3] Kerner B S and Osipov V V 1979 *Fiz. Tekh. Poluprov.* **21** 2342
- [4] Kerner B S and Osipov V V 1989 *Usp. Fiz. Nauk* **157** 201
- [5] Vaschenko I A, Kerner B S and Osipov V V 1989 *Fiz. Tekh. Poluprov.* **23** 1378
- [6] Kerner B S, Litvin D P and Sankin V I 1987 *Pis'ma Zh. Tekh. Fiz.* **13** 819
- [7] Niedernostheide F-J, Kerner B S and Purvins H-G 1992 *Phys. Rev. B* **46** 7559
- [8] Kamilov I K, Stepurenko A A and Kovalyov A S 2000 *Fiz. Tekh. Poluprov.* **34** 433
- [9] Kerner B S and Osipov V V 1985 *Zh. Eksp. Teor. Fiz.* **89** 589
- [10] Vinoslavskiy M N 1989 *Fiz. Tverd. Tela* **31** 315
- [11] Vinoslavskiy M N, Kerner B S, Osipov V V and Sarbei O G 1990 *J. Phys.: Condens. Matter* **2** 2863
- [12] Sarbey O Gand and Vinoslavskiy M N 1994 *Proc. 8th Int. Conf. on 'Hot Carriers in Semicond'* (Oxford, UK, Aug. 1993) ed J Ryan and A Maciel *Semicond. Sci. Technol.* **9** 573
- [13] Sarbey O G, Vinoslavskiy M N and Khizhnyak D A 1995 *Proc. 9th Int. Conf. on 'Hot Carriers in Semicond'* (Chicago, USA, Aug. 1995) ed K Hess et al (New York: Plenum)
- [14] Vinoslavskiy M N and Sarbey O G 1996 *Proc. 23rd Int. Conf. on 'The Physics of Semiconductors'* (Berlin, Germany, July 1996) ed M Scheffler and R Zimmermann p 117
- [15] Sarbey O G, Vinoslavskiy M N and Kravchenko A V 1999 *Ukr. Fiz. Zh.* **44** 190
- [16] Prior A C 1960 *Proc. Phys. Soc.* **76** 465
- [17] Akopyan A A and Gribnikov Z S 1976 *Solid-State Electron.* **19** 41